Iranian Journal of Astronomy and Astrophysics
Vol. 11, No. 2, Spring 2024, 117–132
©Available online at http://ijaa.du.ac.ir
DOI: 10.22128/ijaa.2024.851.1188
Online ISSN: 2383–403X

Iranian Journal of Astronomy and Astrophysics

Research Paper

Unveiling the Universe: Tsallis Holographic Dark Energy and Modified Logarithmic $f(R)$ Gravity

Fatemeh Baziar[1] · Jafar Sadeghi[2]

[1] Department of Physics, Faculty of Basic Sciences, University of Mazandaran P.O.Box 47416–95447, Babolsar, Iran;
email: solalehbaziar70@gmail.com

[2] Department of Physics, Faculty of Basic Sciences, University of Mazandaran P.O.Box 47416–95447, Babolsar, Iran;
email: pouriya@ipm.ir

Received: 11 July 2024; **Accepted:** 27 October 2024; **Published:** 13 November 2024

Abstract. In this paper, we delve into the intricacies of the Tsallis holographic dark energy model within the framework of a modified logarithmic $f(R)$ gravity. This gravity model is distinctive due to its composition, which includes both polynomial terms and a logarithmic component. Our primary objective is to compute the equation of state parameter for the proposed model, which is a crucial step in understanding the behavior of dark energy in the universe. To achieve a comprehensive analysis, we employ two distinct scale factor structures: the exponential and the hybrid. The exponential scale factor is known for its simplicity and relevance in cosmological models that exhibit a constant rate of expansion. On the other hand, the hybrid scale factor offers a more nuanced approach, accommodating both early-time deceleration and late-time acceleration phases of the universe's expansion. Furthermore, we rigorously test the stability of our model. One of the key methods we use is examining the sound speed, which serves as an indicator of the propagation of perturbations through the dark energy field. By plotting various figures, we can visually represent the stability conditions and analyze the viability of the Tsallis holographic dark energy model in a modified gravity context. Lastly, we meticulously document our findings, providing detailed expressions and calculations.

Keywords: Modified logarithmic $f(R)$ gravity, Tsallis holographic dark energy

1 Introduction

Dark energy is a mysterious phenomenon that affects the universe on the largest scales. It is the name given to the unknown cause of the "accelerated expansion" of the universe. Scientists do not know what dark energy is, but they have some possible explanations for it. One is that it is a "property of space" itself, that creates a negative pressure that stretches the fabric of spacetime. Another is that it is a "cosmological constant", a term in Einstein's theory of gravity that represents a constant energy density filling space homogeneously. A third possibility is that it is a "scalar field", a dynamic quantity that varies in time and space and has energy density. According to the current measurements, dark energy makes

up about 70% of the total energy in the observable universe. There are two main types of dark energy: the "cosmological constant" and "scalar fields". The cosmological constant is a constant energy density that fills space homogeneously and does not change over time or space. Scalar fields are dynamic quantities that have energy densities that vary in time and space. Some examples of scalar fields are "quintessence" and "moduli". Quintessence is a scalar field that has a negative pressure and can change over time. Moduli are scalar fields that arise from extra dimensions in string theory and can change over space [1–4].

Dark energy from the perspective of holographic structure has been the focus of researchers. The holographic structure of dark energy is a hypothesis that tries to explain the origin and nature of dark energy using the holographic principle. The holographic principle states that the information content of a region of space can be encoded on a lower-dimensional boundary to that region. This implies that the universe is like a hologram, where a three-dimensional image is projected from a two-dimensional surface. One way to apply the holographic principle to dark energy is to assume that the entropy of the universe is proportional to its horizon area, rather than its volume. This leads to a relation between the energy density of dark energy and the size of the horizon. If the horizon is smaller, the energy density is higher, and vice versa. This can explain why the energy density of dark energy is so low, because the horizon of the observable universe is very large. Another way to apply the holographic principle to dark energy is to assume that the quantum fluctuations of matter and radiation in the universe are constrained by the holographic bound, which limits the amount of information that can be stored in a given region of space. This leads to a relation between the energy density of dark matter and radiation and the size of the horizon. If the horizon is smaller, the energy density is lower, and vice versa. This can explain why the energy density of dark matter and radiation decreases as the universe expands, while the energy density of dark energy remains constant [5,6].

The different structures of dark energy refer to how it affects the formation and evolution of cosmic structures, such as galaxies and clusters of galaxies. Depending on the type and properties of dark energy, it can have different effects on the growth of structures and the distribution of matter in the universe. For example, if dark energy is a cosmological constant, it does not affect the growth of structures until very late times, when it dominates the energy density of the universe and causes the expansion to accelerate. If dark energy is a scalar field, it can affect the growth of structures at earlier times, depending on how it varies over time and space. Some scalar fields can also cause the expansion to decelerate or oscillate, rather than accelerate [7,8]. Some of the methods that scientists use to study the different structures of dark energy are:

"Supernova observations": Supernovae are exploding stars that can be used as standard candles to measure the distance and expansion rate of the universe at different times. By comparing the observed brightness and redshift of supernovae, scientists can infer how dark energy affects the expansion history of the universe [9].

"Cosmic microwave background (CMB) observations": The CMB is the relic radiation from the early universe that fills the sky. By analyzing the temperature and polarization fluctuations of the CMB, scientists can infer how dark energy affects the geometry and matter content of the universe [10].

"Large-scale structure (LSS) observations": The LSS is the distribution of matter and galaxies on large scales in the universe. By measuring the clustering and correlation of galaxies, scientists can infer how dark energy affects the growth and evolution of cosmic structures [11].

"Gravitational lensing observations": Gravitational lensing is the bending of light by gravity. By measuring how light from distant sources is distorted by intervening matter, scientists can infer how dark energy affects the distribution and shape of matter in the

universe.Modified gravity theories are theories that try to explain the observed phenomena of the universe, such as the accelerated expansion, without invoking dark energy. Instead, they modify the theory of general relativity, which is the standard theory of gravity, by introducing new terms or fields in the equations that govern gravity. There are many different types of modified gravity theories, each with its own motivations and predictions [12,13].

One type of modified gravity theory is "$f(R)$ gravity", which replaces the Ricci scalar R in the Einstein-Hilbert action with a more general function $f(R)$. This can lead to different effective equations of motion for gravity, which can mimic dark energy or inflation. Some examples of $f(R)$ gravity models are Starobinsky inflation, Hu-Sawicki model, and Palatini formalism. Another type of modified gravity theory is "scalar-tensor gravity", which adds one or more scalar fields to the gravitational action. These scalar fields can couple to matter or curvature, and can affect the dynamics of gravity and cosmology. Some examples of scalar-tensor gravity models are Brans-Dicke theory, chameleon models, and Galileon models. A third type of modified gravity theory is "Einstein-Aether theory", which introduces a dynamical unit timelike vector field that breaks Lorentz invariance. This vector field can modify the propagation of gravitational waves and light, and can affect the cosmological evolution. Some examples of Einstein-Aether theory models are Khronometric theory, Hořava-Lifshitz gravity, and projectable Hořava-Lifshitz gravity. A fourth type of modified gravity theory is "bimetric theory", which considers two interacting metric tensors that describe two sectors of matter and gravity. This can lead to a massive graviton and a cosmological constant that depend on the interaction between the two metrics. Some examples of bimetric theory models are Hassan-Rosen bimetric theory, dRGT massive gravity, and bigravity [14–16]. The modified logarithmic gravity model is a specific example of $f(R)$ gravity. It is given by the action,

$$S = \int d^4x\sqrt{-g}\left[\frac{R}{2\kappa^2} + \frac{1}{2\kappa^2}\ln\left(\frac{R}{\mu^2}\right)R - V_0\right] + S_m, \tag{1}$$

where $\kappa^2 = 8\pi G$, μ is a constant, V_0 is a cosmological constant, and S_m is the matter action. This model can explain the late-time acceleration of the universe without introducing dark energy, by using the logarithmic correction to the Ricci scalar. The model can also avoid the singularity problem of general relativity, by having a bounce solution in the early universe. The model can also pass the solar system tests of gravity, by satisfying the chameleon mechanism [17].

The modified logarithmic gravity model has some interesting features and predictions, such as: The model can have a de Sitter attractor solution, which means that the universe will asymptotically approach a constant expansion rate in the future. The model can have a phantom phase, which means that the effective equation of state of dark energy can be less than -1, leading to a possible future singularity known as the Big Rip. The model can have a cyclic behavior, which means that the universe can undergo repeated cycles of expansion and contraction, with each cycle having a longer duration than the previous one. The model can have a graceful exit from inflation, which means that the universe can make smooth transition from an inflationary phase to a radiation-dominated phase, without requiring reheating or entropy production [18–20]. The above concepts motivated us to organize the article in the following form:
In section 2, we briefly review the structure of $f(R)$ gravity. In section 3, we introduce the Tsallis holographic dark energy. In section 4, we fully introduce the modified logarithmic $f(R)$ theory of gravity. In section 5, we examine the Tsallis holographic dark energy from the perspective of modified logarithmic $f(R)$ theory of gravity by choosing two scale factors: exponential and hybrid. We compare our results with other works in the literature. In section 6, we summarize and discuss our findings.

2 $f(R)$ Gravity

We want to discuss one of the extended theories of general relativity. Therefore, Einstein Hilbert's Lagrangian is first considered for this extended theory with reference to Ricci's scalar in the following form [18–21],

$$S = \frac{1}{2\kappa}\int f(R)\sqrt{-g}d^4x + S_M. \tag{2}$$

According to the above equation, g determines the metric, (S_M) indicates the action of the matter, and we will also have $(\kappa = 8\pi.G)$. with respect to the variation of Lagrange relative to the metric tensor, $f(R)$ gravity field equations can be obtained,

$$R_{\mu\nu}f'(R) - \frac{1}{2}g_{\mu\nu}f(R) - \nabla_\mu\nabla_\nu f'(R) + g_{\mu\nu}\Box f'(R) = \kappa T_{\mu\nu}, \tag{3}$$

where prime shows differentiation of (R), (∇_μ) related to covariant derivative, $(\Box \equiv \nabla_\mu\nabla^\mu)$ and $(T_{\mu\nu})$ the energy-momentum tensor specified as,

$$T_{\mu\nu} = -\frac{2}{\sqrt{-g}}\frac{\partial S_M}{\partial g_{\mu\nu}}. \tag{4}$$

In this way, Einstein's standard field equations can be written as follows,

$$G_{\mu\nu} = \kappa T_{\mu\nu}. \tag{5}$$

So, with respect to above equation, we will have,

$$T_{\mu\nu} = \frac{\kappa}{f'(R)}(T_{\mu\nu} + T^{eff}_{\mu\nu}). \tag{6}$$

Then

$$T^{eff}_{\mu\nu} = \frac{1}{\kappa}[\frac{1}{2}g_{\mu\nu}(f(R) - f'(R)R) + \nabla_\mu\nabla_\mu f'(R) - g_{\mu\nu}\Box f'(R)]. \tag{7}$$

The effective energy-momentum tensor includes geometrical implications, indicating that the energy conditions cannot be created by it. Its effective energy density is not positive-definite. To check the $f(R)$ gravity field equations (equation 5), the FRW universe is assumed to be flat.

$$ds^2 = -dt^2 + a^2(t)[dr^2 + r^2d\theta^2 + r^2\sin^2\theta d\phi^2]. \tag{8}$$

It should be noted that $\hat{a}$(t) is considered as a scale factor. keeping in mind the absolute fluid as the matter content, which is obtained by the energy-momentum tensor,

$$T^{\mu\nu} = (\rho + p)u^\mu u^\nu + pg^{\mu\nu}. \tag{9}$$

It is possible to derive the equations of the field by having (p) and (ρ), which are sequentially fluid pressure and energy density,

$$H^2 = \frac{1}{3f'(R)}(\kappa\rho + \frac{Rf'(R) - f(R)}{2} - 3H\dot{R}f''(R)), \tag{10}$$

$$2\dot{H} + 3H^2 = -\frac{\kappa}{f'(R)}(p - \frac{Rf'(R) - f(R)}{2} - 2H\dot{R}f''(R) + \dot{R}^2f'''(R) + \ddot{H}f''(R)). \tag{11}$$

The above equations are called Friedman's equations as (11) shows the differentiation of time, and its structure can be written as follows,

$$2\dot{H}+2H^2=-H^2-\frac{\kappa}{f'(R)}(p-\frac{Rf'(R)-f(R)}{2}-2H\dot{R}f''(R)+\dot{R}^2f'''(R)+\ddot{H}f''(R)). \quad (12)$$

By having the equation (10), we will have,

$$\dot{H}+H^2=\frac{\ddot{\hat{a}}}{\hat{a}}=-\frac{\kappa}{6}\rho+\rho_{eff}+3(p+p_{eff}). \quad (13)$$

Then

$$\rho_{eff}=\frac{1}{\kappa f'(R)}(\frac{Rf'(R)-f(R)}{2}-2H\dot{R}f''(R). \quad (14)$$

Also,

$$p_{eff}=\frac{\kappa}{\kappa f'(R)}(\dot{R}^2f'''(R)+\ddot{H}f''(R)-\frac{Rf'(R)-f(R)}{2}+2H\dot{R}f''(R)). \quad (15)$$

We modify equation (13) for the accelerated universe as follows,

$$\rho+\rho_{eff}+3(p+p_{eff})<0\Rightarrow\frac{p+p_{eff}}{\rho+\rho_{eff}}<-\frac{1}{3}. \quad (16)$$

Finally, an equation of state is generated,

$$\omega_{tot}=\frac{p+\dot{R}^2f'''(R)+\ddot{H}f''(R)-\frac{Rf'(R)-f(R)}{2}+2H\dot{R}f''(R)}{\rho+\frac{Rf'(R)-f(R)}{2}-3H\dot{R}f''(R)}. \quad (17)$$

Here, ω_{tot} describes the behavior of the system in the context of $f(R)$ gravity and the construction of matter. By using a specific $f(R)$ model and the field equations, we will study the development of the universe.

3 Tsallis holographic dark energy

First, a summary of the Holographic Dark Energy (HDE) model is provided to help us find the solution to the dark energy. the holographic principle which states that the number of degrees of freedom related to entropy scales directly with the surrounding area of the system [22–24]. The energy density of holography is as follows,

$$\rho=\frac{3c^2M_p^2}{L^2}. \quad (18)$$

It relies on the entropy relation around the black hole, i.e. $S\propto A$, where A is the area of the black hole's event horizon.According to (UV) and (IR) cutoffs [25], a new definition for entropy is provided

$$L^3\Lambda^3=\leq S^{\frac{3}{4}}, \quad (19)$$

where L and Λ are introduced as UV-cutoffs and IR, respectively. By generalizing the standard Boltzmann-Gibbs entropy and converting it to a non-expansive entropy then it can be used in Tsallis entropy. So, it was rewritten as follows,

$$S=\gamma A^{\delta}. \quad (20)$$

In the manner that γ is an unknown constant and δ indicates the non-additivity parameter.By taking the limit of $\gamma = \frac{1}{4G}$ and putting $\delta = 1$, the Bekenstein-Hawking entropy is restored. If we consider the equations (19) and (20), the vacuum energy density is obtained,

$$\rho = BL^{2\delta-4}, \tag{21}$$

where B is an unknown parameter.IR cutoffs are used in various cases, such as the Hubble horizon, event horizon, particle horizon, etc. We use the simplest IR cutoffs, that is ($L = H^{-1}$), and the energy density is written as follows

$$\rho = BH^{4-2\delta}. \tag{22}$$

The parameter δ is related to the dimensions of the system and is defined as $\delta = d/d-1$ and also if we put $d = 1$, holographic dark energy is restored. Now this is if $\delta = 2$ gives us the cosmological constant. Therefore, if we consider the Friedman equation and the equation of state, we will have the conservation of energy as follows,

$$\dot{\rho} + 3H(\rho + p) = 0. \tag{23}$$

Pressure is also calculated as,

$$p = \frac{2\delta - 4}{3} B\dot{H}H^{-2\delta+2} - BH^{-2\delta+4}. \tag{24}$$

4 Modified logarithmic $f(R)$ gravity model

The characteristics of the $f(R)$ gravity model are altered due to conditions and limitations. In this section, we want to give more information about the modified $f(R)$ gravity model, which has a logarithmic term [26–29] that includes logarithmic plus polynomial terms.

$$f(R) = R + \alpha R^2 + \beta R^n + \gamma R^2 \ln \gamma R. \tag{25}$$

It should be noted that neutron stars, cosmic models, and gluon effects can be considered by the logarithmic mode with respect to constant parameters n, α, β, and γ [26–29]. we will have,

$$\begin{aligned} f'(R) &= 1 + (2\alpha + \gamma)R + 2\gamma R \ln \gamma R + n\beta R^{n-1}, \\ f''(R) &= 2\alpha + \gamma + 2\gamma \ln \gamma R + n(n-1)\beta R^{n-2}. \end{aligned} \tag{26}$$

Equations (25) and (26) are very important so that the gravitational model can be introduced by them provided that we set the parameters α, β and γ. If $\beta = 0$, it shows the Starobinski model. $\gamma = 0$ and $n = 4$ studied in [26–29]. with $f(0) = 0$ one condition is met in $f(R)$, which shows a smooth spacetime without cosmic constant. as well as the stability of this model has been fully investigated in [26–29]. So, having the above model, the quantum stability situations is compatible with $f(R)$ and the classical stability condition is obtained.

$$f'(R) = 1 + (2\alpha + \gamma + 2\gamma \ln \gamma R)R + n\beta R^{n-1} > 0. \tag{27}$$

5 Discussion and results

We will study a model of dark energy that is based on two ideas: the holographic principle and the Tsallis entropy. The holographic principle says that the information in a space is

related to the area of its boundary, not its volume. The Tsallis entropy is a way of measuring the disorder of a system that can deal with non-standard situations, such as long-range forces or fractal shapes. The model assumes that the dark energy density depends on the Hubble horizon and the Tsallis parameter, which shows how much the entropy differs from the usual one. This model can explain why the universe is expanding faster and faster without using a cosmological constant or a scalar field. We also used a modified version of $f(R)$ gravity theory, which is a way of changing Einstein's theory of gravity by using a different function of the Ricci scalar, R, in the action. The modified version has a polynomial and a logarithmic term in the function. This version can describe the early inflation and the late-time acceleration of the universe. We used two different ways of describing how the universe grows with time. One way was exponential, which means that the growth rate is constant. The other way was hybrid, which combines an exponential and a power-law term, which allows for a change from slowing down to speeding up.

5.1 Exponential case

According to the above equations, we calculate the energy density and pressure for the logarithmic model for the exponential case ($\hat{a} = t^a$), which are in the following form,

$$\rho_{exp} = \frac{3a(2a-1)\left(36a^2(4a(a+1)-3)\gamma(2\alpha+3\gamma)-t^4\right)+a\beta\gamma 6^{n+1}(n-1)t^4(2a+2n-1)\left(\frac{a(2a-1)}{t^2}\right)^n}{2\gamma t^2\left(\beta 6^n n t^4\left(\frac{a(2a-1)}{t^2}\right)^n-6a(2a-1)\left(t^2-6a(2a-1)(2\alpha+3\gamma)\right)\right)}, \tag{28}$$

and

$$\begin{aligned} P_{exp} =& -\frac{12a^4(6a+5)(2\alpha+3\gamma)}{(2a-1)t^4}+\frac{12a^3(6a+5)(2\alpha+3\gamma)}{(2a-1)t^4}-\frac{3a^2(6a+5)(2\alpha+3\gamma)}{(2a-1)t^4} \\ &+\frac{\beta 2^{n-1}3^{n-2}(n-1)nt\left(\frac{a(2a-1)}{t^2}\right)^n}{(1-2a)^2a}+\beta 6^{n-1}(n-1)\left(\frac{a(2a-1)}{t^2}\right)^n \\ &\left(4n\left(\frac{6(n-2)t^2}{\beta 6^n n t^4\left(\frac{a(2a-1)}{t^2}\right)^n-6a(2a-1)\left(t^2-6a(2a-1)(2\alpha+3\gamma)\right)}+\frac{1}{1-2a}\right)-3\right) \\ &+\frac{a(4\alpha+6\gamma)}{t^3}+\frac{1}{4\gamma}. \end{aligned} \tag{29}$$

Using the above two equations as well as the explanations given in detail in the previous sections, we can fully calculate some quantities such as the equation of state, which is specified in section Appendix A. One possible method of measuring the stability of dark energy models using the speed of sound is to study the effects of dark energy perturbations on the cosmic microwave background (CMB) and the matter power spectrum. Dark energy perturbations are characterized by the sound speed parameter, c_s^2, which determines how fast the dark energy density and pressure fluctuations propagate in the medium. If c_s^2 is different from the speed of light, then dark energy perturbations can grow or decay over time and distance, depending on the equation of state and the background expansion rate. This can affect the CMB temperature and polarization anisotropies, as well as the clustering of matter on large scales. To measure the sound speed parameter, one can use a combination of CMB and large-scale structure data, such as galaxy surveys or weak lensing measurements. By comparing the theoretical predictions of different dark energy models with different values of c_s^2 with the observed data, one can constrain the sound speed parameter and test the stability of dark energy models. For example, one can use a Bayesian analysis

to compute the likelihood function and the posterior distribution of c_s^2 given the data and a prior distribution. Alternatively, one can use a frequentist approach to calculate the chi-square statistic and the confidence intervals of c_s^2 given the data and a fiducial model. Some previous studies have applied this method to various dark energy models, such as quintessence, phantom, k-essence, or early dark energy models. They have found that current data can put only weak constraints on the sound speed parameter, but future data may be able to improve the sensitivity and distinguish between different dark energy models. So, the sound speed is given by,

$$c_s^2 = \frac{dp/dt}{d\rho/dt}, \tag{30}$$

According to the above explanation as well as equations (28) and (29) and with respect to the relationship of sound speed, we can discuss the stability of the above model, the results of which are briefly shown in the figs. As Figure 1 shows, the equation of state as a function of time is plotted for different values of n, which is the power of the term of logarithmic model. The equation of state is a measure of the pressure and density of the cosmic fluid, and it can be used to describe the evolution of the universe. The figure also displays the variation of the equation of state with respect to n in Figure (1b). This variation shows how the equation of state changes as n increases or decreases, and how it affects the expansion rate of the universe. Moreover, the stability of the logarithmic model for an exponential case is illustrated in Figure (1c). The logarithmic model is a modified gravity theory that can explain the accelerated expansion of the universe without invoking dark energy. The figure includes different free parameters as indicated in the figures.. As it is known, positive values imply stability and negative values imply instability of the system. The stability and instability regions of the model are clearly marked in Figure (1c). These regions indicate whether the model can produce consistent and realistic cosmological solutions or not. In Figure 2, the equation of state as a function of n is drawn for different values of the Tsallis parameter, and these variations are clearly shown in the figure. The figure shows how different values of this parameter affect the equation of state and hence the expansion history of the universe.

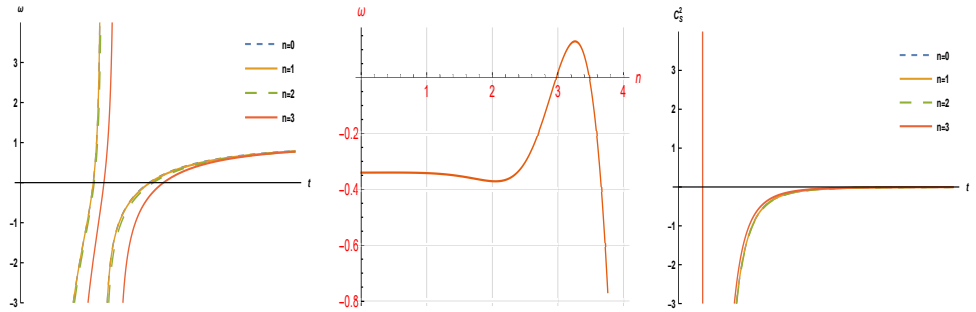

(a) (b) (c)

Figure 1: The plot of the $\omega - t$ for different values of n in fig (1a), plot of the $\omega - n$ in fig (1b) and the plot of the stability determined in fig (1c) with respect to $\alpha = 0.15, \beta = 0.009, \gamma = 0.01$, and $a = 1$

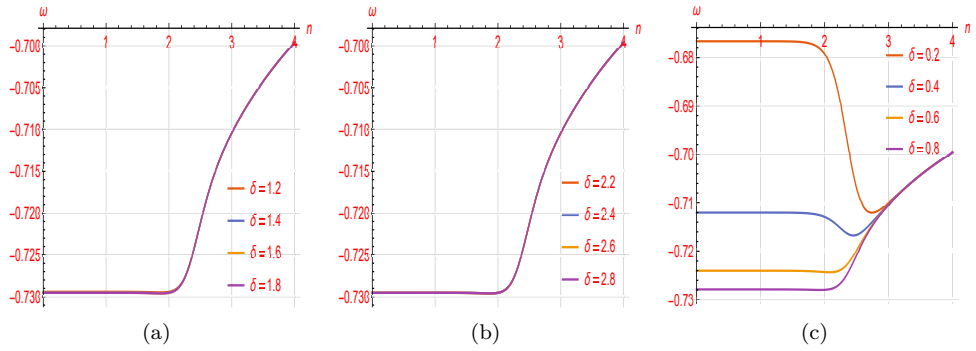

(a) (b) (c)

Figure 2: The plot of the ω in terms of n with respect to different values of δ and $a = 1$

5.2 Hybrid case

Also, we proposed the same trend for the logarithmic model for the hybrid scale factor ($\hat{a} = e^{ct}t^{b}$). As we explained in the previous section, we perform similar calculations for the hybrid case of the logarithmic model. The calculations related to this section are included in Appendix B and we discuss the results here in detail.

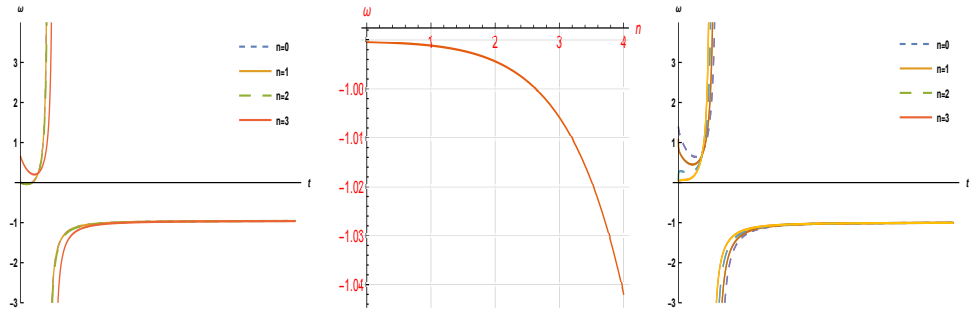

(a) (b) (c)

Figure 3: The plot of the $\omega - t$ for different values of n in fig (3a), plot of the $\omega - n$ in fig (3b) and the plot of the $\omega - t$ for different values of n and $\delta = 0.5$ determined in fig (3c) with respect to $\alpha = 0.15, \beta = 0.009, \gamma = 0.01$, $c = 1.5$, and $b = 0.5$

As Figure 3 shows, the equation of state as a function of time is plotted for different values of n, which is the power of the term of logarithmic model. The equation of state is a measure of the pressure and density of the cosmic fluid, and it can be used to describe the evolution of the universe. The figure also displays the variation of the equation of state with respect to n in Figure (3b). This variation shows how the equation of state changes as n increases or decreases, and how it affects the expansion rate of the universe. Also, the equation of state as a function of time is plotted for different values of n and δ in Figures (3c), (4a), and (4b). δ is a dimensionless parameter. The figures show how different values of δ influence the equation of state and hence the acceleration or deceleration of the universe. Moreover, the stability of the logarithmic model for a Hybrid case is illustrated in Figure (4c). The Hybrid case is a combination of exponential and power-law scale factors that

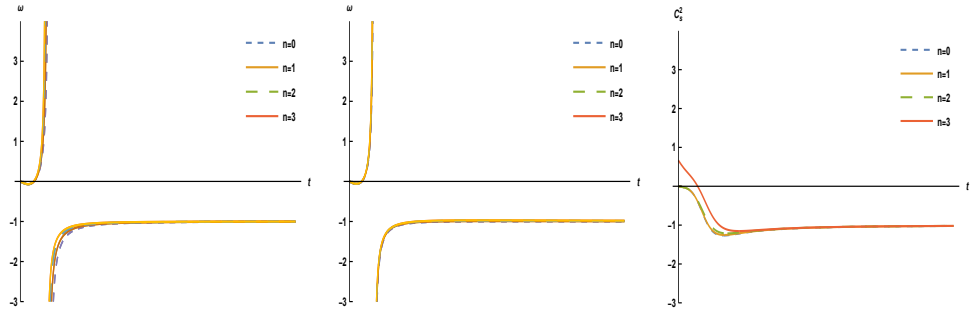

(a) (b) (c)

Figure 4: The plot of the $\omega - t$ for different values of n and $\delta = 1.5$ and $\delta = 2.5$ in fig (4a) and (4b) and the plot of the stability determined in fig (4c) with respect to $\alpha = 0.15, \beta = 0.009, \gamma = 0.01$ $c = 1.5$, and $b = 0.5$

can mimic different phases of the universe. The figure includes different free parameters as indicated in the figures. As it is known, positive values imply stability and negative values imply instability of the system. The stability and instability regions of the model are clearly marked in Figure (4c) with respect to different values of n. These regions indicate whether the model can produce consistent and realistic cosmological solutions or not.

6 Conclusion

The Tsallis holographic dark energy was investigated in this paper using a modified logarithmic $f(R)$ gravity model that consisted of a polynomial and a logarithmic part. The Tsallis holographic dark energy is a generalization of the standard holographic dark energy that incorporates non-extensive statistics and non-additive entropy. The modified logarithmic $f(R)$ gravity model is a modified gravity theory that can explain the accelerated expansion of the universe without invoking dark energy. The equation of state for our model was calculated using two scale factor structures: exponential and hybrid. The scale factor is a function that describes how the size of the universe changes with time. The exponential scale factor represents a de Sitter phase of the universe, while the hybrid scale factor represents a combination of exponential and power-law phases that can mimic different epochs of the universe. The equation of state for our model shows how the pressure and density vary with time and depend on the free parameters of the model. The stability of our model was also checked using the sound speed and the results were plotted in figures. The sound speed can indicate whether the model is stable or unstable. The figures show how the sound speed changes with time and with different values of the free parameters. Finally, our results were expressed in details. Our results show that our model can produce realistic cosmological solutions that are consistent model and that our model can avoid some of the problems that plague other models of dark energy.

Appendix A: Calculation of the equation of state for the exponential case

Therefore, according to the above two equations (28) and (29), the equation of state for the mentioned model can be calculated as,

$$A_1 = 2^n 3^{n+1} ant^6 \beta((2(6^n(n-1)(4n-3)\beta(\frac{a(2a-1)}{t^2})^n + 6p)\gamma + 3)t^2$$

$$A_2 = 4(n-1)\gamma t + 48(n-2)(n-1)\gamma)(\frac{a(2a-1)}{t^2})^n + 2^{2n+1}9^n(n-1)n^2t^9\beta^2\gamma(\frac{a(2a-1)}{t^2})^{2n}$$

$$A_3 = -746496a^{11}\gamma(2\alpha+3\gamma)^2 + 1244160a^{10}\gamma(2\alpha+3\gamma)^2 + 10368a^8\gamma(2\alpha+3\gamma)(-7t^2+8\alpha t-120\alpha+12(t-15)\gamma)$$

$$A_4 = +62208a^9\gamma(2\alpha+3\gamma)(t^2-5(2\alpha+3\gamma)) + 432a^5((2(6^n(n-1)(\frac{a(2a-1)}{t^2})^n\beta - 2p)\gamma - 1)t^6$$

$$A_5 = +6(2\alpha+3\gamma)(6^n(n(4n-9)+6)\beta\gamma(\frac{a(2a-1)}{t^2})^n + 12p\gamma + 3)t^4 + 12\gamma(2\alpha+3\gamma)t^3 - 51\gamma(2\alpha+3\gamma)t^2$$

$$A_6 = -48\gamma(2\alpha+3\gamma)^2t + 45\gamma(2\alpha+3\gamma)^2) + 6a^2t^5(-2^{n+1}3^n\beta(48t\gamma n^3 + 2\gamma((t-78)t-6\alpha-9\gamma)n^2$$

$$A_7 = +3t^3n + t(2t(6pt-1)+117)\gamma n - 9t\gamma)(\frac{a(2a-1)}{t^2})^n - 4^{n+1}9^n(n-1)n(2n-3)t^3\beta^2\gamma(\frac{a(2a-1)}{t^2})^{2n})$$

$$A_8 = +9t(4p\gamma+1) + 5184a^7(2\alpha+3\gamma)((-6^n(3n-2)\beta\gamma(\frac{a(2a-1)}{t^2})^n + 4p\gamma + 1)t^4 - 2\gamma t^2$$

$$A_9 = -16\gamma(2\alpha+3\gamma)t + 105\gamma(2\alpha+3\gamma)) + 1728a^6(2\alpha+3\gamma)(2(-6^n(n(2n-9)+6) \beta\gamma(\frac{a(2a-1)}{t^2})^n - 12p\gamma - 3)t^4$$

$$A_{10} = -2\gamma t^3 + 27\gamma t^2 + 36\gamma(2\alpha+3\gamma)t - 99\gamma(2\alpha+3\gamma)) + 36a^3t^3(6^nt\beta(nt^4 + 3(n(-8n(t-3) - 27) + 18)\gamma^2 + 2((n(2pt^2 + 8(n-4)n + 33) - 9)t^2$$

$$A_{11} = +(n(-8n(t-3)-27)+18)\alpha)\gamma)(\frac{a(2a-1)}{t^2})^n - 2^{2n+1}9^n(n-1)nt^5\beta^2\gamma(\frac{a(2a-1)}{t^2})^{2n}$$

$$A_{12} = +12\gamma(2\alpha+3\gamma) - 9t^3(4p\gamma+1) + 9t(2\alpha+3\gamma)(4p\gamma+1)) + 72a^4t(2^{n+1}3^nt^3\beta\gamma(2t(2\alpha+3\gamma)n^2 + (n-1)(4n-9)t^2 - 18(n(2n-3)+2)(2\alpha+3\gamma))(\frac{a(2a-1)}{t^2})^n$$

$$A_{13} = +9((4p\gamma+1)t^5 - 4(2\alpha+3\gamma)(4p\gamma+1)t^3 - 4\gamma(2\alpha+3\gamma)t^2 + 5\gamma(2\alpha+3\gamma)t + 4\gamma(2\alpha+3\gamma)^2))$$

$$B_1 = 18a(t-2at)^2(2^{n+1}3^nt^4\beta\gamma(n\rho t^2 + 3a(n-1)(2a+2n-1))(\frac{a(2a-1)}{t^2})^n + 3a(2a-1)(-((4\gamma\rho+1)t^4)$$

$$B_2 = 24a(2a-1)\gamma(2\alpha+3\gamma)\rho t^2 + 36a^2(4a(a+1)-3)\gamma(2\alpha+3\gamma)))$$

$$\omega_{exp} = \frac{A_1 + A_2 + \cdots + A_{13}}{B_1 + B_2}$$

According to the above explanations and equations (22) and (25), the equation of state will be calculated in the following form for an exponential case,

$$C_1 = -144a^8\gamma(36(2\alpha+3\gamma)(\frac{a}{t})^{2\delta} + B) + 48a^7\gamma(72(2\alpha+3\gamma)(\frac{a}{t})^{2\delta} + B(7-2\delta))$$

$$+12a^6\gamma(216(2\alpha+3\gamma)(\frac{a}{t})^{2\delta}+B(8\delta-19))+24a^5\gamma(12(t-9)(2\alpha+3\gamma)(\frac{a}{t})^{2\delta}-B(\delta-2))$$
$$-36a^4(\frac{a}{t})^{2\delta}(-15\gamma(2\alpha+3\gamma)+t^4(\beta\gamma 2^{n+1}3^n(n-1)(\frac{a(2a-1)}{t^2})^n-1)+8\gamma t(2\alpha+3\gamma))$$
$$-12a^3t(\frac{a}{t})^{2\delta}(t^3(\beta\gamma 2^{n+1}3^n(n-1)(2n-3)(\frac{a(2a-1)}{t^2})^n+3)-6\gamma(2\alpha+3\gamma))$$
$$+3a^2t^4(\frac{a}{t})^{2\delta}(\beta\gamma 2^{n+1}3^n(n-1)(4n-3)(\frac{a(2a-1)}{t^2})^n+3)$$
$$+\beta\gamma(-2^{n+1})3^n(n-2)(n-1)nt^7(\frac{a(2a-1)}{t^2})^n(\frac{a}{t})^{2\delta}+a\beta\gamma 2^{n+1}3^n(n-1)nt^5(\frac{a(2a-1)}{t^2})^n(\frac{a}{t})^{2\delta}$$

$$D_1=9a^2(2a-1)(4a^2(2a-1)\gamma(a^2B+9(2a-1)(2a+3)(2\alpha+3\gamma)(\frac{a}{t})^{2\delta})$$
$$+t^4(\frac{a}{t})^{2\delta}(\beta\gamma 2^{n+1}3^n(n-1)(2a+2n-1)(\frac{a(2a-1)}{t^2})^n-2a+1))$$

$$\omega_{exp}(\text{Tsallis})=\frac{C_1}{D_1}$$

Appendix B: Calculation for the hybrid case

Therefore, according to the above explanations, the energy density and pressure for the mentioned model are calculated in the following form

$$E_1=\frac{4b^2\beta(n-2)(n-1)n(2b+2ct-1)^2(\frac{2(b+ct)^2-b}{t^2})^n}{(4bct+b(2b-1)+2ct^2)^3}$$
$$-\frac{(2(b+ct)^2-b)(\beta n(\frac{4bct+b(2b-1)+2ct^2}{t^2})^{n-1}+\frac{(2\alpha+3\gamma)(4bct+b(2b-1)+2ct^2)}{t^2}-1)}{2t^2}$$
$$-\frac{4b(\frac{b}{t}+c)(2b+2ct-1)(2\alpha+\frac{\beta(n-1)nt^4(\frac{4bct+b(2b-1)+2ct^2}{t^2})^n}{(4bct+b(2b-1)+2ct^2)^2}+3\gamma)}{t^3}$$
$$+\frac{1}{4}(2\beta(\frac{4bct+b(2b-1)+2ct^2}{t^2})^n$$
$$+\frac{(4bct+b(2b-1)+2ct^2)((2\alpha+3\gamma)(4bct+b(2b-1)+2ct^2)-2t^2)}{t^4}+\frac{1}{\gamma})$$
$$+\frac{2b(2\alpha+\frac{\beta(n-1)nt^4(\frac{4bct+b(2b-1)+2ct^2}{t^2})^n}{(4bct+b(2b-1)+2ct^2)^2}+3\gamma)}{t^3}$$

$$F_1=\beta n(\frac{4bct+b(2b-1)+2ct^2}{t^2})^{n-1}+\frac{(2\alpha+3\gamma)(4bct+b(2b-1)+2ct^2)}{t^2}-1$$

$$P_H=\frac{E_1}{F_1}$$

and

$$G_1=6b(\frac{b}{t}+c)(2b+2ct-1)(2\alpha+\frac{\beta(n-1)nt^4(\frac{4bct+b(2b-1)+2ct^2}{t^2})^n}{(4bct+b(2b-1)+2ct^2)^2}+3\gamma)$$

$$G_2=t^3(\beta n(\frac{4bct+b(2b-1)+2ct^2}{t^2})^{n-1}+\frac{(2\alpha+3\gamma)(4bct+b(2b-1)+2ct^2)}{t^2}-1)$$

$$H_1=2\beta(\frac{4bct+b(2b-1)+2ct^2}{t^2})^n$$

$$+\frac{(4bct+b(2b-1)+2ct^2)((2\alpha+3\gamma)(4bct+b(2b-1)+2ct^2)-2t^2)}{t^4}+\frac{1}{\gamma}$$

$$H_2=4(\beta n(\frac{4bct+b(2b-1)+2ct^2}{t^2})^{n-1}+\frac{(2\alpha+3\gamma)(4bct+b(2b-1)+2ct^2)}{t^2}-1)$$

$$\rho_H=\frac{G_1}{G_2}-\frac{b-2(b+ct)^2}{2t^2}-\frac{H_1}{H_2}$$

According to the above two equations, the equation of state is obtained as,

$$I_1=\frac{16b^2(n-2)(n-1)n(2b+2ct-1)^2\beta(\frac{2(b+ct)^2-b}{t^2})^n}{(2ct^2+4bct+b(2b-1))^3}$$
$$+2(\frac{b(2b-1)}{t^2}+c(\frac{4b}{t}+2))^n\beta+\frac{8b(\frac{(n-1)nt^4\beta(\frac{b(2b-1)}{t^2}+c(\frac{4b}{t}+2))^n}{(2ct^2+4bct+b(2b-1))^2}+2\alpha+3\gamma)}{t^3}$$
$$+\frac{(2ct^2+4bct+b(2b-1))((2ct^2+4bct+b(2b-1))(2\alpha+3\gamma)-2t^2)}{t^4}$$
$$-\frac{2(2(b+ct)^2-b)(n\beta(\frac{b(2b-1)}{t^2}+c(\frac{4b}{t}+2))^{n-1}+\frac{(2ct^2+4bct+b(2b-1))(2\alpha+3\gamma)}{t^2}-1)}{t^2}$$
$$-\frac{16b(\frac{b}{t}+c)(2b+2ct-1)(\frac{(n-1)nt^4\beta(\frac{b(2b-1)}{t^2}+c(\frac{4b}{t}+2))^n}{(2ct^2+4bct+b(2b-1))^2}+2\alpha+3\gamma)}{t^3}+\frac{1}{\gamma}$$

$$I_2=4(n\beta(\frac{b(2b-1)}{t^2}+c(\frac{4b}{t}+2))^{n-1}+\frac{(2ct^2+4bct+b(2b-1))(2\alpha+3\gamma)}{t^2}-1)$$

$$I_3=2\beta(\frac{b(2b-1)}{t^2}+c(\frac{4b}{t}+2))^n$$
$$+\frac{(2ct^2+4bct+b(2b-1))((2ct^2+4bct+b(2b-1))(2\alpha+3\gamma)-2t^2)}{t^4}+\frac{1}{\gamma}$$

$$I_4=4(n\beta(\frac{b(2b-1)}{t^2}+c(\frac{4b}{t}+2))^{n-1}+\frac{(2ct^2+4bct+b(2b-1))(2\alpha+3\gamma)}{t^2}-1)$$

$$I_5=6b(\frac{b}{t}+c)(2b+2ct-1)(\frac{(n-1)nt^4\beta(\frac{b(2b-1)}{t^2}+c(\frac{4b}{t}+2))^n}{(2ct^2+4bct+b(2b-1))^2}+2\alpha+3\gamma)$$

$$I_6=t^3(n\beta(\frac{b(2b-1)}{t^2}+c(\frac{4b}{t}+2))^{n-1}+\frac{(2ct^2+4bct+b(2b-1))(2\alpha+3\gamma)}{t^2}-1)$$

$$\omega_H=p+\frac{I_1}{I_2}-\frac{I_3}{I_4}+\frac{I_5}{I_6}+\rho-\frac{b-2(b+ct)^2}{2t^2}$$

Similar to the previous subsection, this time also according to equations (22) and (25), the equation of state for the model in the hybrid scale factor example is calculated in the following form, and we also discussed the stability of the model, which is clearly shown in the figs.

$$J_1=\frac{4b^2\beta(n-2)(n-1)n(2b+2ct-1)^2(\frac{2(b+ct)^2-b}{t^2})^n}{(4bct+b(2b-1)+2ct^2)^3}$$
$$-\frac{2bB(\delta-2)(\frac{b}{t}+c)^{2-2\delta}}{3t^2}$$
$$-B(\frac{b}{t}+c)^{4-2\delta}+\frac{2b(2\alpha+\frac{\beta(n-1)nt^4(c(\frac{4b}{t}+2)+\frac{b(2b-1)}{t^2})^n}{(b(2b+4ct-1)+2ct^2)^2}+3\gamma)}{t^3}$$

$$+\frac{1}{4}-\frac{2(2(b+ct)^2-b)(\beta n(c(\frac{4b}{t}+2)+\frac{b(2b-1)}{t^2})^{n-1}+\frac{(2\alpha+3\gamma)(4bct+b(2b-1)+2ct^2)}{t^2}-1)}{t^2}$$
$$+2\beta(c(\frac{4b}{t}+2)+\frac{b(2b-1)}{t^2})^n$$
$$+\frac{(4bct+b(2b-1)+2ct^2)((2\alpha+3\gamma)(4bct+b(2b-1)+2ct^2)-2t^2)}{t^4}$$
$$+\frac{1}{\gamma}-\frac{4b(\frac{b}{t}+c)(2b+2ct-1)(2\alpha+\frac{\beta(n-1)nt^4(c(\frac{4b}{t}+2)+\frac{b(2b-1)}{t^2})^n}{(4bct+b(2b-1)+2ct^2)^2}+3\gamma)}{t^3}$$

$$J_2=B(\frac{b}{t}+c)^{4-2\delta}+\frac{1}{4}\frac{2(2(b+ct)^2-b)(\beta n(c(\frac{4b}{t}+2)+\frac{b(2b-1)}{t^2})^{n-1}+\frac{(2\alpha+3\gamma)(4bct+b(2b-1)+2ct^2)}{t^2}-1)}{t^2}$$
$$-2\beta(c(\frac{4b}{t}+2)+\frac{b(2b-1)}{t^2})^n$$
$$-\frac{(4bct+b(2b-1)+2ct^2)((2\alpha+3\gamma)(4bct+b(2b-1)+2ct^2)-2t^2)}{t^4}$$
$$-\frac{1}{\gamma}+\frac{4b(2b+2ct-1)(\frac{b}{t}+c)(2\alpha+\frac{\beta(n-1)nt^4(c(\frac{4b}{t}+2)+\frac{b(2b-1)}{t^2})^n}{(4bct+b(2b-1)+2ct^2)^2}+3\gamma)}{t^3}$$

$$\omega_H(\text{Tsallis})=\frac{J_1}{J_2}$$

Authors' Contributions

All authors have the same contribution.

Data Availability

The data that support the findings of this study are available from the corresponding author upon reasonable request.

Conflicts of Interest

The authors declare no potential conflicts of interest.

Ethical Considerations

The authors have diligently addressed ethical concerns, such as informed consent, plagiarism, data fabrication, misconduct, falsification, double publication, redundancy, submission, and other related matters.

Funding

This research did not receive any grant from funding agencies in the public, commercial, or nonprofit sectors.

References

[1] Lin, MX., McDonough, E., Hill, JC., & Hu, W. 2023, Phys. Rev. D, 107, 103523.

[2] Zhao, ZW., Wang, LF., Zhang, JG., Zhang, JF., & Zhang, X. 2023, J. Cosmology Astropart. Phys., 2023, 022.

[3] Saridakis, EN., Yang, W., Pan, S., Anagnostopoulos, FK., & Basilakos, S. 2023, Nucl. Phys. B, 986, 116042.

[4] Finster, F., & Isidro, JM. 2023, Classical and Quantum Gravity, 40, 075017.

[5] Fusco, M. P. 2023, Black Hole Entropy and the Holographic Universe. In The Physics and Metaphysics of Transubstantiation, Springer.

[6] Anchordoqui, L. A., Barger, V., Marfatia, D., & Soriano, J. F. 2022, APS, 105, 103512.

[7] Vogelsberger, M., Marinacci, F., Torrey, P., & Puchwein, E. 2020, Nature Reviews Physics, 2, 42.

[8] Abbott, T. M. C., Aguena, M., Alarcon, A., Alves, O., Amon, A., & et al. 2023. Phys. Rev. D, 107, 083504.

[9] Holanda, R. F. L., Colaço, L. R., Pereira, S. H., & Silva, R. 2019, J. Cosmology Astropart. Phys., 2019, 008.

[10] Komatsu, E. 2022, Nature Reviews Physics, 4, 452.

[11] Ivanov, M. M., McDonough, E., Hill, J. C., Simonovic, M., Toomey, M. W., & et al. 2020, Phys. Rev. D, 102, 103502.

[12] Kuang, X. M., Tang, Z. Y., Wang, B., & Wang, A. 2022, Phys. Rev. D, 106, 064012.

[13] Oguri, M. 2019, Reports on Progress in Physics, 82, 126901.

[14] Harko, T., Myrzakulov, N., Myrzakulov, R., & Shahidi, S. 2021, Physics of the Dark Universe, 34, 100886.

[15] Parbin, N., & Goswami, U. D. 2021, Modern Physics Letters A, 36, 2150265.

[16] Böhmer, C. G., & Jensko, E. 2021, Phys. Rev. D, 104, 024010.

[17] Odintsov, S. D., & Nojiri, S. 2006, ECONF C, 602061, 06.

[18] Granda, L. 2020, Symmetry, 12, 794.

[19] Paliathanasis, A., Said, J. L., & Barrow, J. D. 2018, Phys. Rev. D, 97, 044008.

[20] Casas, S., Pauly, M., & Rubio, J. 2018, Phys. Rev. D, 97, 043520.

[21] Ens, P. S., & Santos, A. F. 2020, Europhysics Letters, 131, 40007.

[22] Yan, H. 2019, Phys. Rev. B, 99, 155126.

[23] Sadeghi, J., Noori Gashti, S., & Azizi, T. 2023, Modern Physics Letters A, 2350076.

[24] Sadeghi, J., Gashti, S. N., & Azizi, T. 2023, Communications in Theoretical Physics, 75, 025402.

[25] Cantcheff, M. B., Gadelha, A. L., Marchioro, D. F., & Nedel, D. L. 2018, The European Physical Journal C, 78, 1.

[26] Sadeghi, J., Pourhassan, B., Noori Gashti, S., Naghd Mezerji, E., & Pasqua, A. 2022, Universe, 8, 623.

[27] Sadeghi, J., Shokri, M., Gashti, S. N., Pourhassan, B., & Rudra, P. 2022, International J. Modern Physics D, 31, 2250019.

[28] Sadeghi, J., & Gashti, S. N. 2021, Pramana, 95, 1.

[29] Sadeghi, J., Mezerji, E. N., & Gashti, S. N. 2021, Modern Physics Letters A, 36, 2150027.

[30] Rej, P., Bhar, P., & Govender, M. 2021, The European Physical Journal C, 81, 316.